processes

MDPI

Article

Safety-Oriented Coordinated Operation Algorithms for Natural Gas Pipeline Networks and Gas-Fired Power Generation Facilities

Xinyi Wang [1,*], Feng Wang [1], Qin Bie [1], Wenlong Jia [2], Yong Jiang [3], Ying Liu [1], Yuanyuan Tian [1], Yuxin Zheng [2] and Jie Sun [2]

[1] Institute of Gathering and Transportation Engineering Technology, PetroChina Southwest Oil & Gas Field Company, Chengdu 610040, China
[2] School of Oil & Natural Gas Engineering, Southwest Petroleum University, Chengdu 610500, China
[3] Gas Field Development and Management Department, PetroChina Southwest Oil & Gas Field Company, Chengdu 610056, China
* Correspondence: wangxinyi1995@petrochina.com.cn

Abstract

The natural gas pipeline network transmission system involved in the coordinated operation of pipeline networks and gas-fired power generation facilities is complex. It consists of multiple components, such as gas sources, users, valves, compressor stations, and pipelines. The addition of natural gas-fired power generation facilities overlaps with the high and low peak periods of civil gas, imposing dual peak-shaving pressures on pipeline networks and requiring more stringent operational control strategies for maintaining system stability. To address the aforementioned issues and improve the overall operating revenues of the system, we proposed the coordinated optimization model of gas-fired power generation facilities, pipeline networks, gas storage, and compressor stations. The optimization algorithm is written using the penalty function method of the Interior Point OPTimizer (IPOPT) solver. Meanwhile, the basic parameters of the system's pipeline networks, users, gas storage, natural gas-fired power generation facilities, compressors, and electricity prices were input into the solver. The research results reveal that the algorithm ensures solution accuracy while accounting for computational efficiency and practical applicability. The algorithm can be used to effectively calculate the ideal coordinated operation solution, significantly improve the operating revenues of the system, and achieve safe, stable, coordinated, and efficient operation of the system.

Keywords: gas-fired power generation facility; optimization model; interior point OPTimizer; coordinated operation

check for updates

Academic Editor: Jie Zhang

Received: 30 April 2025
Revised: 29 June 2025
Accepted: 2 July 2025
Published: 8 July 2025

Citation: Wang, X.; Wang, F.; Bie, Q.; Jia, W.; Jiang, Y.; Liu, Y.; Tian, Y.; Zheng, Y.; Sun, J. Safety-Oriented Coordinated Operation Algorithms for Natural Gas Pipeline Networks and Gas-Fired Power Generation Facilities. *Processes* **2025**, *13*, 2184. https://doi.org/10.3390/pr13072184

Copyright: © 2025 by the authors. Licensee MDPI, Basel, Switzerland. This article is an open access article distributed under the terms and conditions of the Creative Commons Attribution (CC BY) license (https://creativecommons.org/licenses/by/4.0/).

1. Introduction

The coordinated operation optimization technology of pipeline networks and gas-fired power generation facilities aims to enhance efficiency based on the variations in the supply and demand of electricity and natural gas while incorporating the fluctuations in intraday peak and off-peak electricity prices and the constant intraday natural gas prices, along with the characteristics of the pipeline network system. At its core, this technology is based on developing reasonable gas injection and withdrawal strategies for gas storage and optimizing power generation across multiple gas-fired power generation facilities. By doing so, it enhances overall system efficiency, synchronizes the peak shaving capabilities

of gas storage and pipeline networks, and ensures the efficient and coordinated operation of both gas networks and the power grids. Previous studies have thoroughly investigated the steady-state operation optimization in natural gas pipelines [1–7]. However, this study addresses a multi-entity coordination challenge, integrating gas storage peak-shaving, natural gas power plants, and gas pipeline networks. Consequently, it is imperative to conduct a comprehensive investigation and an in-depth analysis into transient optimization technologies for natural gas pipeline systems domestically and internationally.

In 2013, Zavala [8] et al. established a cost-minimization objective function that incorporates compressor operational energy, supply deficit penalties, and pipeline capacity violation penalties. To address the uncertainty of user demand, the researchers developed a two-stage stochastic optimization model, which was subsequently solved using the IPOPT solver, version 3.14.13. Subsequently, in 2016, Zhang [9] et al. concentrated on minimizing the fuel consumption in compressor stations along pipelines. In their research, dynamic programming (DP) was utilized to approximate transient processes as a series of steady-state time intervals (1 h), and experiments were performed on the Central Asian natural gas pipeline. In 2017, Ahmadian [10] formulated an optimization framework aimed at minimizing the energy consumption of compressor stations along pipeline networks. To tackle uncertain factors, the author employed chance-constrained programming and scentless transformation and established an optimization model containing uncertain factor constraints. In 2021, Baum [11] et al. introduced a two-stage iterative solution algorithm designed for transient optimization of natural gas pipeline networks. In 2022, Wen [12] et al. constructed an integrated infrastructure planning model of the natural gas pipeline network that synergizes flow distribution with the optimization goal of minimizing total costs. In 2023, Wen [13] et al. further took into account various pipeline elements, such as bidirectional pipeline networks, multi-pipeline structures, gas storage, and compressors, and coupled the hydraulic calculation equations with linear processing to boost the rationality of the flow distribution scheme. In 2023, Hong [14] designed a two-stage relaxation optimization algorithm to incorporate the thermal process into the hydraulic calculation, thereby improving the accuracy of the hydraulic calculation and making the natural gas transmission scheme more suitable for engineering applications. In 2024, Wen [15] et al. studied the rules and mechanisms of pipeline network capacity configuration, with a focus on the natural gas pipeline network system.

Concerning solution algorithms for optimization models, both dynamic programming [16–18] and the gradient method [19–21] demonstrate significant limitations when applied to large-scale complex pipeline networks, as they rely on initial solutions and undergo large amounts of computation. While the enhanced complex method [22–24] demonstrates a superior solution performance for certain problems, it may face issues such as slow convergence and a tendency to fall into local optimality when applied to high-dimensional models. The hybrid genetic annealing algorithm [25–27] can effectively avoid premature convergence, but its high computational complexity limits its real-time performance and economic feasibility in industrial applications. In contrast, the IPOPT solver method offers robust, strong numerical stability and convergence, proving its computational efficiency and potential for practical application. Accordingly, the IPOPT solver method was selected in this study to optimize the operation of natural gas pipeline networks. The gas–electricity co-optimization model involves complex nonlinear constraints and objective functions, such as the limitations of the inherent operational capacity of gas storage facilities and the processing capacity constraints of the compressor in the optimization model. The IPOPT solver can ensure an accurate and stable solution is found. Meanwhile, the IPOPT solver supports a wide range of optimization problem forms, including continuous optimization, discrete optimization, and mixed-integer optimization.

This flexibility enables it to deal with various types of gas-power co-optimization problems, whether considering goals such as minimizing power generation costs or maximizing the benefits of gas-power projects.

To sum up, there is no transient optimization algorithm that considers gas power, the network, and gas storage at the same time, and there is also no optimization algorithm that considers the optimal economic benefits under the condition of ensuring safety for the following areas. Building upon this foundation, we comprehensively considered the coordinated operation optimization among multiple subjects, such as peak shaving of gas storage and power generation of natural gas power plants.

2. Optimization Model of Coordinated Operation of Pipeline Networks and Gas-Fired Power Generation Facilities

2.1. Objective Function

In this optimization model, the objective function is set to maximize the overall operating earnings of the pipeline network system, as expressed in Equation (1).

$$\min F = f_1 - f_2 - f_3 \tag{1}$$

Firstly, the revenues of gas-fired power generation facilities are derived from natural gas sales to multiple gas-fired power generation facilities. It corresponds to the sales revenues generated under time-varying commercial gas prices throughout the day, as shown in Equation (2).

$$f_1 = \sum_{t \in T} \sum_{i \in N^e} pr_t^{gas} q_{i,t}^{d} \tau \tag{2}$$

where N^e refers to the set of gas and power project nodes; pr_t^{gas} refers to the natural gas price during time period t, CNY/m^3; $q_{i,t}^{d}$ indicates the offtake volume at node i and time t, m/s; and τ is the time step, s.

Secondly, the operating costs of compressor stations primarily consist of power consumption costs during station operation and the transmission tariff for gas injection into the national pipeline network. The calculation incorporates two categories of compressors: electric motor-driven compressors and natural gas turbine-driven compressors, as seen in Equation (3):

$$f_2 = \sum_{t \in T} \sum_{i \in N^c} pr^{gas} \frac{N_{i,t}^{gas}}{H} \tau + pr_t^{elc} N_{i,t}^{elc} \tau + q_{i,t}^{load} \tau \; pr^{load} \tag{3}$$

where N^c is the set of compressor station nodes; $N_{i,t}^{gas}$ refers to the power of the gas turbine-driven compressor at station i during time period t, kW; $N_{i,t}^{elc}$ indicates the power of the electric motor-driven compressor at station i during time period t, kW; $q_{i,t}^{load}$ refers to the injection flow rate into the national pipeline network at node i during time t, m^3/s; and pr^{load} denotes the transmission tariff for pipeline injection, CNY/m^3.

Thirdly, the injection and production costs of gas storage primarily consist of the electricity consumption for compressor operation during gas injection and material expenses for dehydration treatment during gas production, as shown in Equation (4).

$$f_3 = \sum_{t \in T} \sum_{i \in N^{st}} pr_t^{elc} \; N_{i,t}^{st} \tau + pr_i^{wd} q_{t,i}^{s} \tau \tag{4}$$

where N^{st} indicates the set of gas storage nodes; pr_i^{wd} represents the average gas production costs of gas storage i; $q_{t,i}^{s}$ denotes the injection volume of node i during time period t.

2.2. Decision Variable

Several key issues shall be addressed when formulating daily operation schemes for the integrated pipeline, gas storage, and gas-fired power generation facility system. They include coordinating the generation dispatch of multiple gas-fired power generation facilities, scheduling the injection-withdrawal capacity of multiple gas storage facilities, and optimizing the injection volume of the compressor stations connected to the national pipeline network. Thus, the gas injection and production volume of the gas storage facility, the pressure ratio of the compressor station, and the power generation of the gas power project are set as decision variables. By making reasonable decisions on these issues, the best operation scheme is sought under the condition of satisfying the gas demand and operation constraints of users and new gas power projects, as shown in Equation (5).

$$X = \left[\begin{bmatrix} q^{d}_{1,1}, \ldots, q^{d}_{1,i}, \ldots, q^{d}_{1,N^e} \\ q^{d}_{2,1}, \ldots, q^{d}_{2,i}, \ldots, q^{d}_{2,N^e} \\ \ldots \\ q^{d}_{T,1}, \ldots, q^{d}_{T,i}, \ldots, q^{d}_{T,N^e} \end{bmatrix} \begin{bmatrix} q^{load}_{1,1}, \ldots, q^{load}_{1,j}, \ldots, q^{load}_{1,N^c} \\ q^{load}_{2,1}, \ldots, q^{load}_{2,j}, \ldots, q^{load}_{2,N^c} \\ \ldots \\ q^{load}_{T,1}, \ldots, q^{load}_{T,j}, \ldots, q^{load}_{T,N^c} \end{bmatrix} \begin{bmatrix} q^{d/s}_{1,1}, \ldots, q^{d/s}_{1,k}, \ldots, q^{d/s}_{1,N^{st}} \\ q^{d/s}_{2,1}, \ldots, q^{d/s}_{2,k}, \ldots, q^{d/s}_{2,N^{st}} \\ \ldots \\ q^{d/s}_{T,1}, \ldots, q^{d/s}_{T,k}, \ldots, q^{d/s}_{T,N^{st}} \end{bmatrix} \right] \tag{5}$$

2.3. Key Constraints

1. Constraints on the injection-withdrawal volume of gas storage: As shown in Equations (6)–(9), during the gas injection period, if the operating state of gas storage is $x^{st}_i = 1$, the constraint Equations (6) and (9) take effect; if the operating state of gas storage during the gas withdrawal period is $x^{st}_i = 0$, the constraint Equations (7) and (8) take effect. While maintaining compliant injection-withdrawal volumes, gas storage restricts the pipeline injection volume to zero during storage injection phases and the pipeline withdrawal volume to zero during storage withdrawal phases. In practical operations, gas storage typically sustains either injection or withdrawal states for prolonged duration. Thus, our intraday optimization model excludes transitions between injection and withdrawal states.

$$q^{in,\min}_i + M\left(x^{st}_i - 1\right) \le q^{d}_{i,t} \le q^{in,\max}_i + M\left(1 - x^{st}_i\right), i \in N^{st}, t \in T \tag{6}$$

$$q^{wd,\min}_i - Mx^{st}_i \le q^{s}_{i,t} \le q^{wd,\max}_i + Mx^{st}_i, i \in N^{st}, t \in T \tag{7}$$

$$-Mx^{st}_i \le q^{d}_{i,t} \le Mx^{st}_i, i \in N^{st}, t \in T \tag{8}$$

$$M\left(x^{st}_i - 1\right) \le q^{s}_{i,t} \le M\left(1 - x^{st}_i\right), i \in N^{st}, t \in T \tag{9}$$

where $q^{in,\min}_i$ and $q^{in,\max}_i$ denotes the minimum and maximum injection rates of gas storage i, m^3/s; M means a sufficiently large value; x^{st}_i represents the operation status parameter of gas storage (1 for injection period, 0 for withdrawal period); $q^{wd,\min}_i$ and $q^{in,\max}_i$ indicates the minimum and maximum withdrawal rates of gas storage i, m^3/s; N^{st} refers to the set of gas storage nodes.

2. Gas consumption constraints for gas-fired power generation facilities: the optimization model incorporates operation constraints for gas-fired power generation facilities, determined by the actual gas demand of end-users and technical operation constraints inherent to gas-fired power generation facilities.

In terms of user demand, the power generation capacity of gas-fired power generation facilities should fully consider the generation conditions of other power generation sources such as hydropower and coal power at different times within the 24 h across seasons, as well as user electricity consumption and absorption capacity, and reasonably determine the operation constraints of the power generation capacity of gas-fired power generation

facilities, as shown in Equation (10). This constraint guarantees the safe and stable operation of the equipment and prevents situations of overload or inefficient operation. This factor shall be taken into account in the optimization model to reasonably arrange the operating status of the units and ensure that the equipment operates within a safe range.

Moreover, essential devices in gas-fired power generation facilities, including gas turbines, waste heat boilers, steam turbines, etc., are subjected to upper and lower output limits. The output of these devices must not fall below the minimum stable load or above the maximum design capacity as indicated in Equation (11).

$$W_{i,t} = q_{i,t}^{d} H \eta_i^e \tau, i \in N^e, t \in T \tag{10}$$

$$W_{i,t}^{\min} \le W_{i,t} \le W_{i,t}^{\max}, i \in N^e, t \in T \tag{11}$$

where $W_{i,t}$ refers to the power generation capacity of the gas-fired power generation facility i during time period t, kWh. $W_{i,t}^{\min}$ and $W_{i,t}^{\max}$ refer to the minimum and maximum power generation capacities of gas-fired power generation facility i during time period t, kWh.

2.4. Model Summary

Based on the basic situation of the Sichuan–Chongqing natural gas pipeline network and gas-fired power generation facilities and the analysis results of operation optimization, the model aims to maximize the overall economic benefits of natural gas pipeline networks and gas-fired power generation facilities. We fully considered the coordinated operation relationship among pipeline networks, gas storage, and gas-fired power generation facilities and set the gas injection and withdrawal volume of gas storage. The pressure ratio of compressor stations and the power generation capacity of gas-fired power generation facilities are regarded as decision variables. Constraints are set around the operating characteristics of six core parts: gas sources, users, gas storage clusters, compressor stations, pipelines, and gas-fired power generation facilities, so that the final solution can meet the actual operational needs of the system and ensure a long-term efficient and stable operation state.

The coordinated operation optimization model of pipeline networks, gas-fired power generation facilities, and gas storage is formally characterized in a generalized formulation comprising an objective function, an equality constraint, and an inequality constraint, as shown in Equations (12)–(14):

$$\min f(x) \tag{12}$$

$$S.t.\ h_i(x) = 0,\ i = 1, 2 \ldots, M \tag{13}$$

$$g_j(x) \le 0,\ j = 1, 2, \ldots, L \tag{14}$$

where $f(x)$ indicates the general form of the objective function; $h_i(x)$ denotes the equality constraint; M is the number of equality constraints; $g_j(x)$ represents the inequality constraint; and L refers to the number of inequality constraints.

This optimization model is constructed based on the basic situation of the Sichuan–Chongqing natural gas pipeline network and gas-fired power generation facilities and the analysis results of operation optimization. It sought to maximize the overall economic benefits of natural gas pipeline networks and gas-fired power generation facilities. On the premise of ensuring the safety of equipment and pipelines, we considered the power generation revenues of the gas-fired power generation facilities, the operating energy consumption of the compressor stations, and the injection-withdrawal costs of gas storage so as to seek an ideal operation scheme, which maximizes the operational benefits of pipeline networks and gas-fired power generation facilities.

3. Algorithm Design and Robustness Analysis

3.1. Controller Design

IPOPT, an open-source code characterized by robust features and high expansibility, is widely used to implement the nonlinear interior point method. In this project, we used it to solve the coordinated optimization model proposed herein.

The interior point method is an algorithm designed for solving linear and nonlinear optimization problems. It distinctly outperforms conventional gradient methods (such as the Newton method or quasi-Newton method) in handling large-scale optimization problems. Generally speaking, the interior point method constructs a barrier function on the constraint boundary, ensuring all its iteration points are located inside the feasible region. To be specific, the interior point method calculates the optimal solution x^* in turn after comparing a series of $\{x(r_k)\}$ inside the feasible region. Thus, the method is also referred to as the barrier function method and the interior penalty function method. It is applicable to solving optimization problems with only inequality constraints (no equality constraints). The problem formulation is as shown in Equation (15):

$$\begin{aligned} &\min f(x) \\ &\text{s.t. } g_i(x) \geq 0 (i = 1, 2, \ldots, m) \end{aligned} \tag{15}$$

where $f(x)$, $g_i(x)$ is a continuous function, and its domain of definition is $S = \{x | g_i(x) \geq 0, i = 1, 2, \ldots, m\}$. Pursuant to the principle of the interior point method, the auxiliary equation is as shown in Equation (16):

$$F(x, y) = f(x) + \gamma B(x) \tag{16}$$

where γ is the penalty factor, and its value is a sufficiently small number greater than zero; $B(x)$ is the barrier function. When the value of x tends to the limit of the feasible region $B(x) \to \infty$, $B(x)$ can be expressed in two forms, as shown in Equation (17):

$$B\left(x\right) = -\sum_{i=1}^{m} \log c_i\left(x\right) \text{ or } B\left(x\right) = \sum_{i=1}^{m} \frac{1}{c_i\left(x\right)} \tag{17}$$

Further, we can get $F(x, \gamma) \to \infty$. Based on the definition form of $B(x)$ and the property of being sufficiently small of γ, it can be seen that if the value of the function $F(x, \gamma)$ is close to $f(x)$, then the smaller the γ value, the closer the optimal solution of the above problem is to the optimal solution of the original constraint problem, according to the properties of the barrier function. As shown in Equation (18),

$$\lim_{\gamma \to 0} F(x, \gamma) = f(x) and \lim_{\gamma \to 0} x(\gamma) = x^* \tag{18}$$

In the above equation, $x(\gamma)$ refers to the minimal point sequence of $F(x, \gamma)$. Given an allowable error $\varepsilon > 0$, the iteration steps of the interior point algorithm are illustrated in Table 1.

Table 1. Iteration steps of the interior point method.

Steps	Procedure
1	Given an initial value x^0, initial penalty factor M_1, penalty factor magnification factor C, set $K = 1$;
2	Using the iteration point x^{k-1} as the initial point, solve the unconstrained optimization problem $F(x, M_k)$ to yield the local minimum x^k;
3	If $(x^k, f(x^k)), M_k\alpha(x) < \varepsilon$, the termination condition is met and x^k is the optimal solution to the original problem, output x^k and stop iteration; otherwise, go to Step 4;
4	Let $M_{k+1} = CM_k, k = k + 1$, go to Step 2.

The internal penalty function method features notable advantages, as all its iteration points are within the feasible region. Each iteration step may not achieve the exact optimum of the constrained problem, but it can obtain an approximate optimal solution. For simple optimization problems, it is probable that the iteration point stays within the feasible region. Nevertheless, while solving complex optimization problems, an algorithm for identifying feasible initial points is required in the presence of multiple variables and constraints.

3.2. The Robustness and Computational Time of the Algorithm

In natural gas pipeline network optimization, the choice of solver directly impacts algorithm convergence, computational efficiency, and robustness. This study employs IPOPT as the core solver due to its exceptional performance in nonlinear programming problems. The feasibility of IPOPT for the optimization of natural gas networks is verified through numerical experiments driven by actual SCADA data, and a comparative analysis is conducted with other solvers.

The high-pressure natural gas pipeline network in this area is modeled. Based on SCADA data, the reliability of the proposed optimization algorithm is verified under the uncertainty of the actual SCADA system. The boundary conditions for setting up the regional pipeline network are as follows: the number of nodes is 10 to 50, the working pressure range is 4.0 to 5.2 MPa, and the gas supply volume is less than or equal to the maximum capacity and must meet the user's demands.

To demonstrate IPOPT's superiority, the following solvers are tested: Constrained Optimization (CONOPT), version 4.10 (GAMS, Washington, DC, USA); Knitro for AMPL (KNITRO), version 13.4 (Artelys, Paris, France); Bonmin, version 1.10.0. The experimental results are analyzed as follows.

As shown in Tables 2–4, IPOPT achieves the highest convergence rate at all scales and remains above 90%. The computing time of IPOPT is the shortest, among which the computing time of the 50-node network is 11.6 s. IPOPT remained stable under interference, showing the lowest objective fluctuation of 5.2%. In terms of convergence rate, computing time and robustness analysis, the IPOPT solver is superior to other solvers.

Table 2. Convergence comparison (%).

Scenario	10-Node Convergence	30-Node Convergence	50-Node Convergence
IPOPT	100	97	93
CONOPT	94	88	79
KNITRO	96	91	85
Bonmin	87	74	63

Table 3. Computation time comparison(s).

Scenario	10-Node Convergence	30-Node Convergence	50-Node Convergence
IPOPT	1.3	4.3	11.6
CONOPT	1.7	6.5	17.9
KNITRO	1.5	5.6	14.8
Bonmin	2.9	10.7	29.4

Table 4. Robustness test (30-node network; ±10% pressure disturbance).

Scenario	Max Objective Fluctuation (%)	Constraint Violations (100 Trials)
IPOPT	5.2	3
CONOPT	6.8	8
KNITRO	5.9	6
Bonmin	8.1	11

4. Application of the Optimization Model of Coordinated Operation of Pipeline Networks and Gas-Fired Power Generation Facilities

4.1. Basic Parameters and Operation of the Regional Pipeline Network System

4.1.1. Basic Parameters of the System

Taking the gas injection period of a complex region containing gas-fired power generation facilities, gas storage, compressor stations, and pipeline networks as an example, we validated the coordinated operation optimization model of gas power pipeline network–gas storage developed in this study. As shown in Figure 1, there are 3 gas inlet stations (N1, N2, and N9) and 10 gas supply stations (N1, N3, N4, N5, N6, N7, N8, N9, N10, and N13) in this region, among which N4 is also a booster-enhanced offtake station, namely a compressor station, and N11 and N12 represent Gas Storage A and Gas Storage B, respectively. In summer, the peak gas consumption period of gas-fired power generation facilities refers to the gas injection period of gas storage.

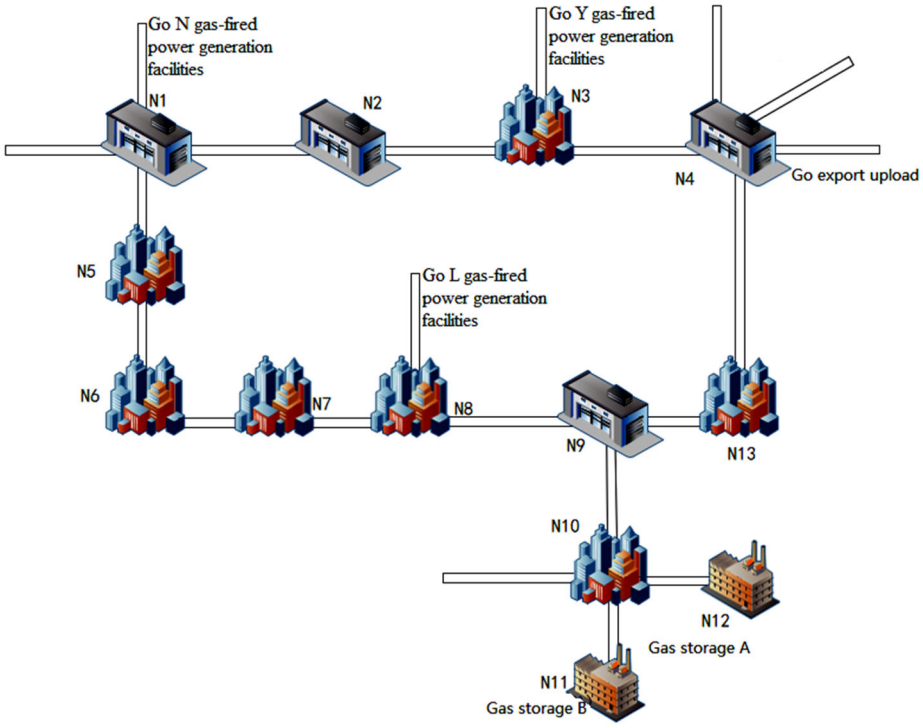


Figure 1. Distribution of regional pipeline networks and stations.

Stations N1-N4 are linked to two gas sources, leading to distinct pipeline flows under varying operating conditions. Accordingly, six possible pipeline flow directions are examined, as seen in Table 5.

Table 5. Flow of regional pipeline networks.

Flow Directions	Contents
Condition 1	(‘N1’, ‘N2’), (‘N2’, ‘N3’), (‘N3’, ‘N4’), (‘N1’, ‘N5’), (‘N5’, ‘N6’), (‘N6’, ‘N7’), (‘N7’, ‘N8’), (‘N8’, ‘N9’), (‘N9’, ‘N10’), (‘N10’, ‘N11’), (‘N10’, ‘N12’), (‘N9’, ‘N13’), (‘N13’, ‘N4’)
Condition 2	(‘N1’, ‘N2’), (‘N2’, ‘N3’), (‘N3’, ‘N4’), (‘N1’, ‘N5’), (‘N5’, ‘N6’), (‘N6’, ‘N7’), (‘N7’, ‘N8’), (‘N9’, ‘N8’), (‘N9’, ‘N10’), (‘N10’, ‘N11’), (‘N10’, ‘N12’), (‘N9’, ‘N13’), (‘N13’, ‘N4’)
Condition 3	(‘N1’, ‘N2’), (‘N2’, ‘N3’), (‘N3’, ‘N4’), (‘N1’, ‘N5’), (‘N5’, ‘N6’), (‘N6’, ‘N7’), (‘N8’, ‘N7’), (‘N9’, ‘N8’), (‘N9’, ‘N10’), (‘N10’, ‘N11’), (‘N10’, ‘N12’), (‘N9’, ‘N13’), (‘N13’, ‘N4’)
Condition 4	(‘N1’, ‘N2’), (‘N2’, ‘N3’), (‘N3’, ‘N4’), (‘N1’, ‘N5’), (‘N5’, ‘N6’), (‘N7’, ‘N6’), (‘N8’, ‘N7’), (‘N9’, ‘N8’), (‘N9’, ‘N10’), (‘N10’, ‘N11’), (‘N10’, ‘N12’), (‘N9’, ‘N13’), (‘N13’, ‘N4’)
Condition 5	(‘N1’, ‘N2’), (‘N2’, ‘N3’), (‘N3’, ‘N4’), (‘N1’, ‘N5’),(‘N6’, ‘N5’), (‘N7’, ‘N6’), (‘N8’, ‘N7’), (‘N9’, ‘N8’), (‘N9’, ‘N10’), (‘N10’, ‘N11’), (‘N10’, ‘N12’), (‘N9’, ‘N13’), (‘N13’, ‘N4’)
Condition 6	(‘N1’, ‘N2’), (‘N2’, ‘N3’), (‘N3’, ‘N4’), (‘N5’, ‘N1’), (‘N6’, ‘N5’), (‘N7’, ‘N6’), (‘N8’, ‘N7’), (‘N9’, ‘N8’), (‘N9’, ‘N10’), (‘N10’, ‘N11’), (‘N10’, ‘N12’), (‘N9’, ‘N13’), (‘N13’, ‘N4’)

4.1.2. Operating Parameters of the System

It is imperative to thoroughly characterize the daily operating conditions of pipeline networks prior to solving the optimal allocation scheme. Such conditions include the initial linepack, prescheduled daily gas injection volume, scheduled gas injection volume from supply sources, time-varying user demand, and initial linepack of pipeline networks. Under such gas injection conditions, the total daily gas injection volume from sources is 26,722,500 m^3/d and the user demand is 16,955,300 m^3/d, respectively. In addition, the scheduled gas injection volume of gas storage is 4,700,000 m^3/d, as shown in Table 6. And the gas storage is subject to the daily gas injection fluctuation limit of 500,000 m^3 to ensure the safe and stable operation of the compressor in the gas storage.

Table 6. Operating condition parameters of gas storage areas.

Name of Gas Storage Areas	Gas Injection Pressure (MPa)	Scheduled Injection Volume (10,000 m^3/d)
A	3.20	220
B	3.00	250

At this time, the three power plants operate simultaneously at peak electricity consumption, with total gas consumption at a rated output ranging from 146,912 m^3/h (3,525,900 m^3/d) to 501,175 m^3/h (12,028,200 m^3/d), as shown in Table 7.

Table 7. Operating condition parameters of natural gas-fired power generation facilities.

Name of Gas-Fired Power Generation Facilities	Maximum Gas Consumption at Rated Output (m^3/h)	Minimum Gas Consumption at Rated Output (m^3/h)
Project N	167,647	41,912
Project L	247,058	61,765
Project Y	86,470	43,235

4.1.3. Gas and Electricity Prices

The region shows considerable spatial variations in both gas and electricity pricing. During the 2024 injection season, the natural gas distribution prices at gate stations along regional pipeline networks were set at 2.12 CNY/m^3. The electricity tariff designates 0.83 CNY/kWh as the baseline rate during normal periods, calibrated at −0.18 CNY/kWh (off-peak periods) and +0.10 CNY/kWh (peak periods).

4.2. Analysis Results of Coordinated Operation of Gas Power Network–Gas Storage

4.2.1. Flow Directions in Pipeline Network Operation During Gas Injection When Gas Storages Are Considered

Following optimization, the flow direction during gas injection in this region is shown in Figure 2, with Stations N1, N2, and N9 serving as gas supply sources to users along the pipeline network. Station N8, which is responsible for supplying the high-demand L gas-fired power generation facility, simultaneously receives a gas supply from both Stations N1 and N9 owing to its substantial consumption requirements. The gas of users along the N1-N9 pipeline segments is mostly supplied by Station N1. Injection demands for N11 (Gas Storage A) and N12 (Gas Storage B) are satisfied by N9. Station N4 receives a concurrent supply of gas from Stations N1, N2, and N9.

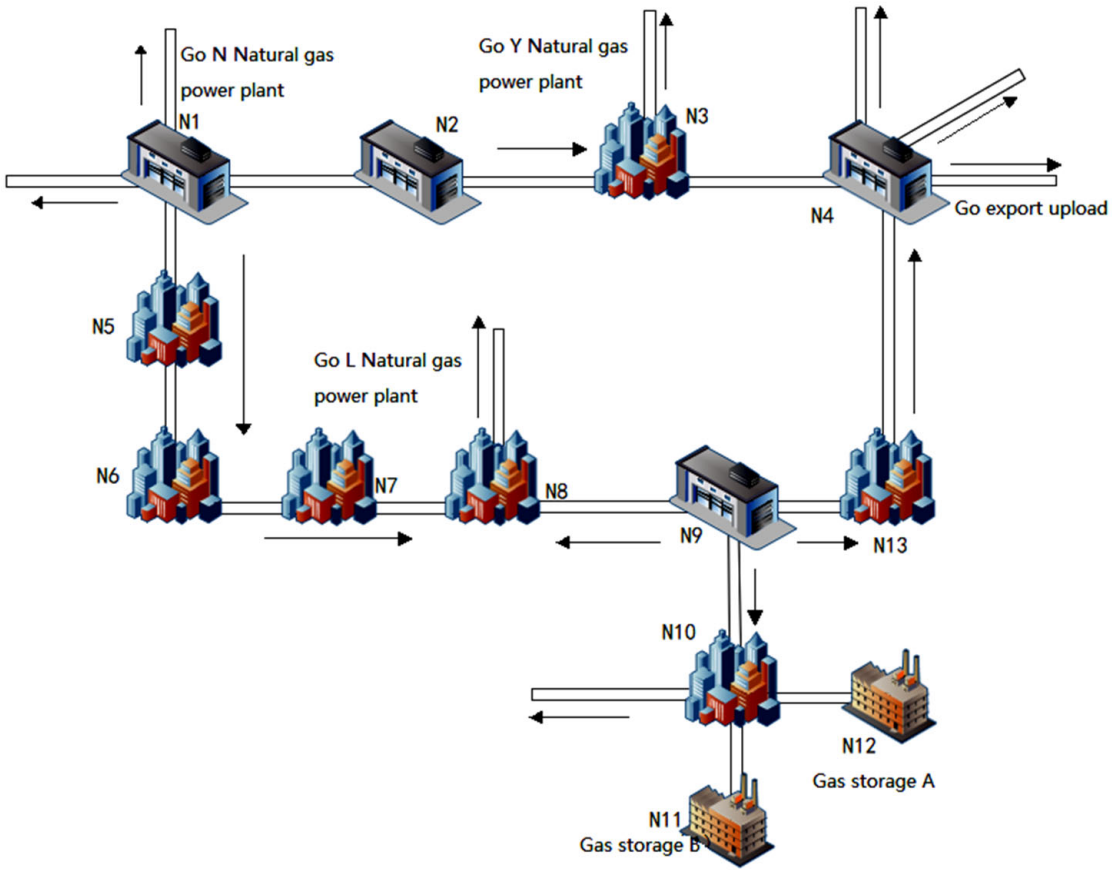


Figure 2. Optimized flow directions during gas injection in the region when gas storages are considered.

4.2.2. Analysis Results

Based on the basic situations of the regional pipeline network, gas storage cluster, and compressor stations, along with the detailed data of gas injection conditions, we empirically applied the Pipeline Network–Gas-Fired Power Generation Facility Coordinated Operation Optimization Model established in this study. Upon its successful implementation, the

system can attain the maximum daily economic revenues of CNY 10,636,200 under the optimal operational conditions. In addition, the total amount of natural gas supplied to the N, L, and Y gas-fired power generation facilities is 5,108,300 m^3/day, as indicated in Table 8.

Table 8. Operating costs and revenues for pipeline networks at different times.

Clock	Gas Sales Revenues for Gas-Fired Power Generation Facilities (CNY)	Offtake and Injection Costs at Station N4 (CNY)	Gas Injection Costs of Gas Storage (CNY)	Total Revenues (CNY)
0:00	352,244	13,186	7788	331,270
1:00	292,289	1561	7874	282,854
2:00	232,335	0	7875	224,460
3:00	182,015	0	7839	174,176
4:00	213,858	0	7777	206,081
5:00	213,858	0	7719	206,139
6:00	248,983	0	7697	241,286
7:00	308,938	0	7648	301,290
8:00	357,432	0	7716	349,716
9:00	447,364	0	7655	439,709
10:00	537,295	0	7652	529,643
11:00	627,227	0	8607	618,620
12:00	717,159	0	8667	708,492
13:00	767,358	0	8743	758,615
14:00	771,112	0	8812	762,300
15:00	711,158	0	8867	702,291
16:00	635,783	0	8973	626,810
17:00	545,851	0	8034	537,817
18:00	472,565	0	8051	464,514
19:00	442,588	0	8077	434,511
20:00	532,520	0	9073	523,447
21:00	502,434	0	9095	493,339
22:00	412,502	0	8113	404,389
23:00	322,570	0	8091	314,479

4.3. Analysis Results of Coordinated Optimization Operation of Gas Power Network

Currently, the gas storage exhibits a limited fluctuation range. Thus, this section will analyze the application of the pipeline network in this region without considering these two gas storage areas, aiming to elucidate the conditions and features of the optimization scheme derived while the gas storage areas are not considered. Simultaneously, an in-depth analysis will be carried out regarding the applicability of the established optimization model for the coordinated operation of the pipeline network system and gas-fired power generation facilities.

4.3.1. Flow Directions in Pipeline Network Operation When Gas Storages Are Not Considered

As shown in Figure 3, when gas storage areas are not considered, the offtake volume from N9 to N10 experiences a reduction, and only the L gas-fired power plant at the N8 and the N9–N4 pipeline segments are unavailable to completely absorb the surplus gas. Accordingly, the flow direction of the from N1 to N9 and N9 to N4 are altered. It shifts from a bidirectional flow (N7/N9 $\rightarrow$ N8), as observed when the gas storages are considered, to a unidirectional flow (N9 $\rightarrow$ N1).

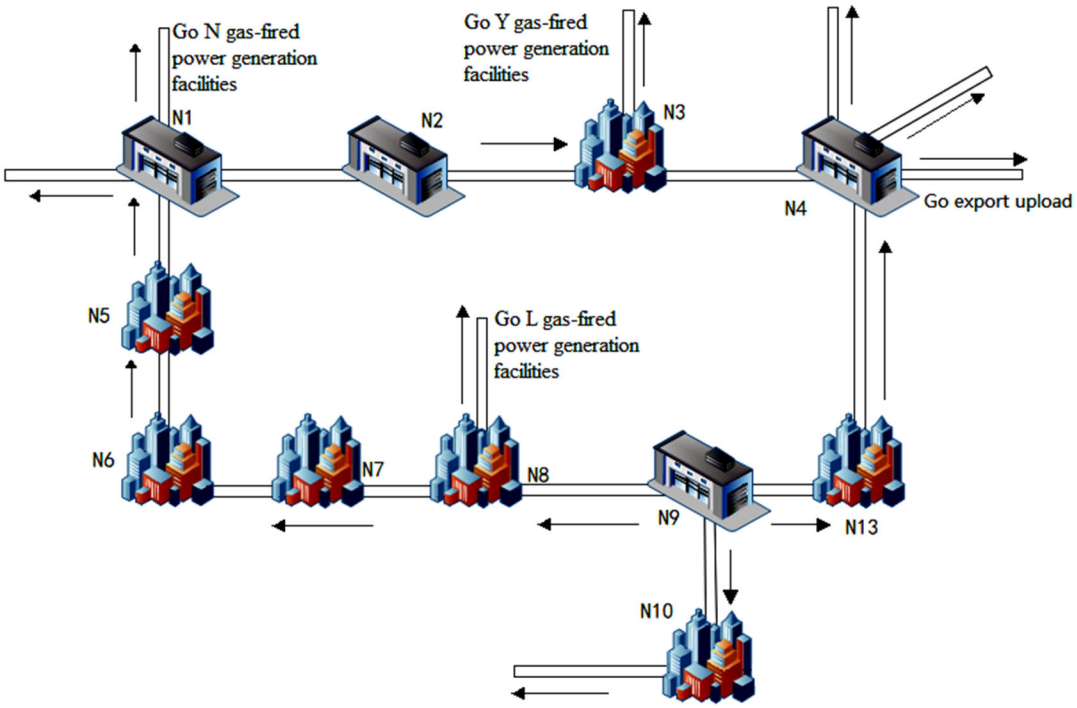


Figure 3. Optimized flow directions during gas injection in the region when gas storage areas are not considered.

4.3.2. Analysis Results

Based on the basic situations, detailed data, and operational condition of pipeline networks, compressor stations, and gas-fired power generation facilities in the southern Sichuan region, we applied the Pipeline Network–Gas-Fired Power Generation Facility Coordinated Operation Optimization Model proposed in this study. Upon solution, the system can achieve maximum daily economic revenues of CNY 16,841,703 under the optimal operation situations, as illustrated in Table 9.

Table 9. Operating costs and revenues of pipeline networks at different times.

Clock	Gas Sales Revenues of Gas-Fired Power Generation Facilities (CNY)	Injection Cost of the Downstream Pipeline of N4 (CNY)	Total Revenues (CNY)
0:00	412,211	25,214	386,997
1:00	442,189	13,564	428,625
2:00	472,166	11,565	460,601
3:00	502,143	11,537	490,606
4:00	532,120	11,507	520,613
5:00	622,052	11,483	610,569
6:00	711,984	11,465	700,519
7:00	801,916	11,455	790,461
8:00	863,747	12,061	851,686
9:00	923,702	12,076	911,626
10:00	953,590	15,455	938,135
11:00	923,613	28,381	895,232
12:00	893,636	24,398	869,238
13:00	863,658	12,518	851,140
14:00	833,681	25,098	808,583
15:00	803,704	37,729	765,975
16:00	773,726	45,461	728,265
17:00	803,704	31,958	771,746
18:00	805,568	19,711	785,857
19:00	805,568	12,298	793,270
20:00	777,436	25,349	752,087
21:00	687,504	22,423	665,081
22:00	597,573	14,070	583,503
23:00	507,641	26,353	481,288

4.4. Contrastive Analysis

4.4.1. Analysis of Changes in Total Gas Consumption for Gas-Fired Power Generation Facilities

This region features a large number of gas-fired power generation facilities, with a broader geographical distribution of users. As a result, there is greater total gas consumption for power generation in gas-fired power generation facilities and more pronounced demand fluctuations. The gas-fired power generation facilities in this region exhibit higher flexibility in peak-shaving and power generation, which in turn undertake heavier peak-shaving tasks and more effectively absorb the surplus gas from supply sources.

Figure 4 illustrates the overall trend of gas consumption for power generation in gas-fired power generation facilities. It can be seen that, when gas storage areas are considered, during off-peak electricity price periods, gas consumption remains comparatively low, fluctuating between 85,715 m^3/h and 165,880 m^3/h. During peak electricity price periods, gas consumption surges to 299,405–361,367 m^3/h. The overall gas consumption changes align with the actual changes in electricity demand and electricity pricing.

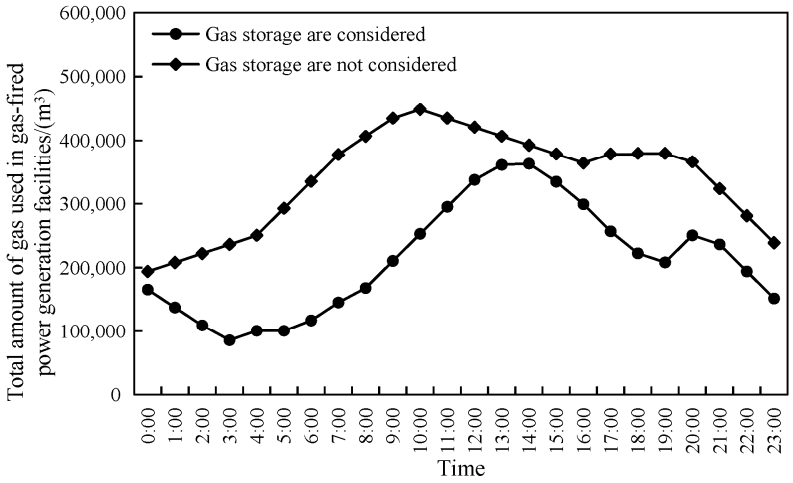


Figure 4. Overall change trend of gas consumption in power generation projects.

When gas storage injection is not considered, gas-fired power plants maintain similar daily electricity consumption. However, gas-fired power plants demonstrate significantly greater gas availability when compared to cases considering gas storage. In this case, all three gas-fired power plants within the pipeline network operate at maximum gas-to-power absorption efficiency, with gas consumption rates between 194,120 m^3/h and 449,068 m^3/h.

4.4.2. Analysis of Changes in Peak-Shaving Volume of Gas Offtake and Injection at Station N4

Figure 5 illustrates that, when gas storage is considered, the majority of peak-shaving and gas surplus absorption tasks in this region are undertaken by multiple gas-fired power generation facilities and the considerable linepack capacity. Consequently, Station N4 carries a relatively minor peak-shaving load and predominantly remains in an injection-idled state. However, in early-day scheduling intervals during periods of substantial supply–demand imbalance, Station N4 injects a restricted volume of gas for peak-shaving purposes. This method results in a sharp reduction in the overall gas offtake and injection costs of the system for peak-shaving purposes.

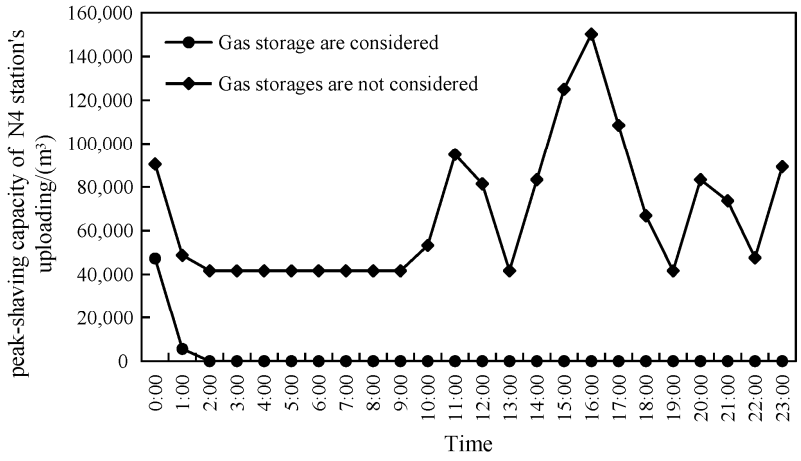


Figure 5. Overall trend of delivery volume at the export point.

When gas storage injection is not considered, the injection volume of the downstream pipeline of N4 increases markedly. During 00:00–10:00 h, the injection volume drops consistently with the increased demand for power from gas-fired power generation facilities. The stepwise variation pattern is formed owing to the constraints on the adjustable fluctuation range of the injection compressor station. The actual injection volume insufficiently satisfies the pipeline network's surplus gas requiring injection. This calls for a tight operational coupling with linepack peak-shaving capacity, resulting in an optimized solution that fully synergizes the linepack peak-shaving capability.

4.4.3. Analysis of Changes in Linepack

In the operation plan within a day, the stock of pipeline pipes also changes constantly within that day. To prevent the optimization model from excessively utilizing the pipe stock for power generation or overly increasing the pipe stock so as to obtain a better solution for the objective function, which would lead to unsafe conditions in the subsequent pipeline operation and not conform to the actual optimization purpose, the pipe stock of the pipeline is restricted to ensure that the pipe stock values are the same at the beginning and end of the day.

Figure 6 illustrates that, when gas storage is considered, due to the larger scale of pipeline networks in this region and their stronger linepack and peak-shaving capacity, they undertake a significant portion of the daily peak-shaving and gas absorption tasks. The overall changes in linepack clearly correspond with the peak and off-peak fluctuations in gas consumption. During the 00:00–08:00 period when gas consumption is low, the linepack exhibits an ascending trend, culminating in a peak of 17,116,152 m^3. Subsequently, during the 09:00–21:00 period, as gas consumption by users and gas-fired power generation facilities increases, the linepack shows a downward trend.

When gas storages are not considered, during the day-start period, gas-fired power plants are in the ramp-up phase. When the injection volume of the National Pipeline Network is low, the linepack shows a continuous upward trend, rising to 16,813,068 m^3 at 7:00. Subsequently, as the gas demand of the gas-fired power plants reaches 377,641–449,068 m^3/h, the linepack shows a declining tendency.

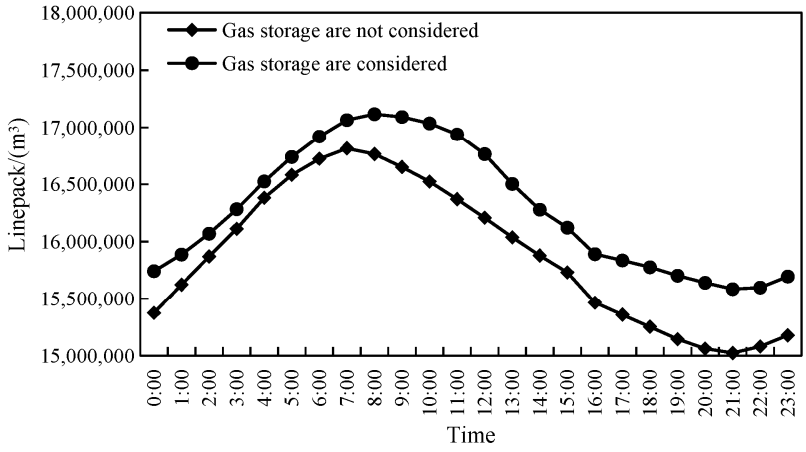


Figure 6. Trend of linepack over time.

4.4.4. Summary

From an economic perspective, if gas storage is not considered, the surplus supply of gas resources is more plentiful, enabling gas-fired power generation facilities to fully leverage their generation capacity for consumption. Consequently, the total power generation revenues increase dramatically. The charge for injecting gas at the export point rises. Nevertheless, the escalation in injection costs is not pronounced in contrast to the substantial increase in economic benefits of the three gas-fired power plants.

The above research demonstrates that this region's greater number and wider distribution of gas-fired power generation facilities enable more flexible and substantial peak-shaving capacity, undertaking the primary peak-shaving tasks. Meanwhile, the pipeline linepack capacity plays a vital role in alleviating daily demand fluctuations by balancing the morning-to-noon peak–off-peak demand difference, working in conjunction with gas-fired power generation facilities to achieve intraday gas consumption peak shaving.

5. Conclusions

This study thoroughly integrated gas-fired power generation facilities, pipeline networks, gas storage, and compressor stations, aiming to maximize the overall economic benefits of natural gas pipeline networks and gas-fired power generation facilities. Utilizing the IPOPT solver, we developed an optimization algorithm to determine the ideal operating strategy that maximizes the total operating revenues of the combined pipeline networks and gas-fired power generation facilities. The effectiveness of this method is verified through a case study of a complex regional gas injection period involving gas-fired power generation facilities, gas storage, compressor stations, and pipeline networks.

(1) Given the significant nonlinearity and high dimensionality of the coordinated optimization model involving natural gas pipeline networks and gas-fired power generation facilities, we comparatively analyzed various optimization solvers to evaluate their advantages, disadvantages, and applicability to the coordinated optimization model. The IPOPT solver is ultimately selected as the primary tool for addressing the optimization problem. It can effectively address the model's high nonlinearity and dimensionality while ensuring computational efficiency and practical feasibility while maintaining solution accuracy.

(2) In this study, an integrated coordinated optimization model is established by focusing on natural gas users, pipeline networks, gas storage, compressor stations, gas sources, and gas-fired power generation facilities. The model sought to identify the optimal coordinated operation strategy while meeting the basic gas and electricity

demands of users and ensuring safe and stable operation of equipment and pipelines, thereby maximizing the system's overall operating benefits and achieving safe, stable, coordinated, and efficient system operations.

(3) A comparative case analysis of this regional pipeline network reveals that the solution results correspond with actual operating conditions and predefined model constraints, yielding significant effects. The coordinated operation optimization technique for pipeline networks and gas-fired power generation facilities, as developed in this study, has proven its favorable applicability in this regional case.

(4) This optimization model relies on the actual gas price, electricity price, and the actual gas consumption of natural gas users in this region and is constrained by the restrictions of this region. In the next step, the above actual values shall be set as range values for the calculation and solution of the optimization algorithm, and this optimization algorithm can be extended to more complex regions.

Author Contributions: Methodology, X.W. and W.J.; Formal analysis, Q.B. and Y.T.; Investigation, F.W.; Resources, Y.Z.; Writing—original draft, F.W.; Writing—review & editing, X.W.; Visualization, Q.B. and J.S.; Supervision, Y.J.; Funding acquisition, Y.L. All authors have read and agreed to the published version of the manuscript.

Funding: This research was funded by the Central Government Guided Local Science and Technology Development Fund Project (2024ZYD0123) and the Major Scientific and Technological Projects of CNPC (2023YQX10503ZK).

Data Availability Statement: The original contributions presented in this study are included in the article. Further inquiries can be directed to the corresponding author.

Conflicts of Interest: Xinyi Wang, Feng Wang, Qin Bie, Yong Jiang, Ying Liu and Yuanyuan Tian were employed by the Petrochina Southwest Oil & Gas Field Company. The remaining authors declare that the research was conducted in the absence of any commercial or financial relationships that could be construed as a potential conflict of interest.

References

1. Kashani, A.H.A.; Molaei, R. Techno-economical and environmental optimization of natural gas network operation. *Chem. Eng. Res. Des.* **2014**, *92*, 2106–2122. [CrossRef]
2. Pratt, K.F.; Wilson, J.G. Optimization of the operation of gas transmission systems. *Trans. Inst. Meas. Control* **1984**, *6*, 261–269. [CrossRef]
3. Sekirnjak, E. Practical experiences with various optimization techniques for gas transmission and distribution systems. In Proceedings of the PSIG Annual Meeting, San Francisco, CA, USA, 23–25 October 1996. PSIG-9603.
4. Rømo, F.; Tomasgard, A.; Hellemo, L.; Fodstad, M.; Eidesen, B.H.; Pedersen, B. Optimizing the Norwegian natural gas production and transport. *Interfaces* **2009**, *39*, 46–56. [CrossRef]
5. Pepper, W.; Ring, B.J.; Read, E.G.; Starkey, S.R. Implementation of a scheduling and pricing model for natural gas. In *Handbook of Networks in Power Systems II*; Springer: Berlin/Heidelberg, Germany, 2012; pp. 3–35.
6. Bermúdez de Castro López-Varela, A.; González Díaz, J.; González Diéguez, F.J.; González Rueda, Á.M.; Pérez Fernández de Córdoba, M. Simulation and optimization models of steady-state gas transmission networks. *Energy Procedia* **2015**, *64*, 130–139. [CrossRef]
7. Žácik, T.; Somora, P.; Hajossy, R. Modeling and optimizing in Slovak gas transmission network. In Proceedings of the PSIG Annual Meeting, Prague, Czech Republic, 16–19 April 2013. PSIG-1319.
8. Zavala, V.M. Stochastic optimal control model for natural gas networks. *Comput. Chem. Eng.* **2013**, *64*, 103–113. [CrossRef]
9. Zhang, X.; Wu, C.; Zuo, L. Minimizing fuel consumption of a gas pipeline in transient states by dynamic programming. *J. Nat. Gas Sci. Eng.* **2016**, *28*, 193–203. [CrossRef]
10. Behrooz, H.A.; Boozarjomehry, R.B. Dynamic optimization of natural gas networks under customer demand uncertainties. *Energy* **2017**, *134*, 968–983. [CrossRef]
11. Hoppmann-Baum, K.; Hennings, F.; Lenz, R.; Gotzes, U.; Heinecke, N.; Spreckelsen, K.; Koch, T. Optimal operation of transient gas transport networks. *Optim. Energy* **2021**, *22*, 735–810. [CrossRef]

12. Wen, K.; Lu, Y.; Lu, M.; Zhang, W.; Zhu, M.; Qiao, D.; Meng, F.; Zhang, J.; Gong, J.; Hong, B. Multi-period optimal infrastructure planning of natural gas pipeline network system integrating flow-rate allocation. *Energy* **2022**, *257*, 124745. [CrossRef]
13. Wen, K.; Qiao, D.; Nie, C.; Lu, Y.; Wen, F.; Zhang, J.; Miao, Q.; Gong, J.; Li, C.; Hong, B. Multi-period supply and demand balance of large-scale and complex natural gas pipeline networks: Economy and environment. *Energy* **2023**, *264*, 126104. [CrossRef]
14. Hong, B.; Qiao, D.; Li, Y.; Sun, X.; Yang, B.; Li, L.; Gong, J.; Wen, K. Supply-demand balance of natural gas pipeline network integrating hydraulic and thermal characteristics, energy conservation and carbon reduction. *Energy* **2023**, *283*, 128427. [CrossRef]
15. Wen, K.; Gao, W.; Hui, X.; Li, L.; Yang, B.; Nie, C.; Miao, Q.; Li, Y.; Li, C.; Hong, B. Allocation of transportation capacity for complex natural gas pipeline networks under fair opening. *Energy* **2024**, *291*, 130330. [CrossRef]
16. Orazbayev, B.; Moldasheva, Z.; Orazbayeva, K.; Makhatova, V.; Kurmangaziyeva, L.; Gabdulova, A. Development of mathematical models and optimization of operation modes of the oil heating station of main oil pipelines under conditions of fuzzy initial information. *East. Eur. J. Enterp. Technol.* **2021**, *6*, 147–162. [CrossRef]
17. Yong, T.; Jefeerson, J.T. Shell pipeline calls it dynamic programming. *Oil Gas J.* **1961**, *59*, 8–12.
18. Gopal, V.N. Optimization pipeline operation. *J. Pet. Technol.* **1980**, *32*, 2063–2067. [CrossRef]
19. Cheng, W.; Liu, Q. Sufficient descent nonlinear conjugate gradient methods with conjugacy condition. *Numer. Algorithms* **2010**, *53*, 113–131. [CrossRef]
20. Neculai, A. Another hybrid conjugate gradient algorithm for unconstrained optimization. *Numer. Algorithms* **2008**, *47*, 143–156.
21. Andrei, N. Hybrid conjugate gradient algorithm for unconstrained optimization. *J. Optim. Theory Appl.* **2009**, *141*, 249–264. [CrossRef]
22. Pandey, H.M.; Chaudhary, A.; Mehrotra, D. A comparative review of approaches to prevent premature convergence in GA. *Appl. Soft Comput.* **2014**, *24*, 1047–1077. [CrossRef]
23. Guria, C.; Bhattacharya, P.K.; Gupta, S.K. Multi-objective optimization of reverse osmosis desalination units using different adaptations of the non-dominated sorting genetic algorithm (NSGA). *Comput. Chem. Eng.* **2005**, *29*, 1977–1995. [CrossRef]
24. Ripon, K.S.N.; Kwong, S.; Man, K.F. A real-coding jumping gene genetic algorithm (RJGGA) for multi-objective optimization. *Inf. Sci.* **2006**, *177*, 632–654. [CrossRef]
25. Roshani, A.; Roshani, A.; Roshani, A.; Salehi, M.; Esfandyari, A. A simulated annealing algorithm for multi-manned assembly line balancing problem. *J. Manuf. Syst.* **2013**, *32*, 238–247. [CrossRef]
26. Roshani, A.; Nezami, F.G. Mixed-model multi-manned assembly line balancing problem: A mathematical model and a simulated annealing approach. *Assem. Autom.* **2017**, *37*, 34–50. [CrossRef]
27. Patriksson, M. *The Traffic Assignment Problem: Models and Methods*; Dover Publications: New York, NY, USA, 2015.

Disclaimer/Publisher's Note: The statements, opinions and data contained in all publications are solely those of the individual author(s) and contributor(s) and not of MDPI and/or the editor(s). MDPI and/or the editor(s) disclaim responsibility for any injury to people or property resulting from any ideas, methods, instructions or products referred to in the content.